

An Efficient Quadratic Penalty Method for a Class of Graph Clustering Problems

Wenshun Teng¹ · Qingna Li^{2,✉}

Received: date / Accepted: date

Abstract Community-based graph clustering is one of the most popular topics in the analysis of complex social networks. This type of clustering involves grouping vertices that are considered to share more connections, whereas vertices in different groups share fewer connections. A successful clustering result forms densely connected induced subgraphs. This paper studies a specific form of graph clustering problems that can be formulated as semi-assignment problems, where the objective function exhibits block properties. We reformulate these problems as sparse-constrained optimization problems and relax them to continuous optimization models. We apply a quadratic penalty method to the relaxation problem and solve the nonlinear quadratic penalty subproblem with simple box constraints using a projected gradient method based on the active set. Extensive numerical results indicate that our method provides more accurate clustering results for solving graph clustering problems at a faster speed, both for synthetic graphs and real-world network datasets, particularly in large-scale cases.

Keywords Graph clustering · Network community detection · Sparse optimization · Quadratic penalty method · Projected gradient method · Semi-assignment problems

The corresponding author's research is supported by NSFC 12071032 and NSFC 12271526

✉ Qingna Li
E-mail: qnl@bit.edu.cn
School of Mathematics and Statistics/Beijing Key Laboratory on MCAACI, Beijing Institute of Technology, Beijing, China

¹ Wenshun Teng
E-mail: teng-wenshun@163.com
School of Mathematics and Statistics, Beijing Institute of Technology, Beijing, China

Mathematics Subject Classification (2020) 90C10 · 90C20 · 90C27 · 05C90

1 Introduction

The community-based graph clustering problem [1], also known as network community detection, is one of the most popular topics in the analysis of complex networks. It has widespread applications in various fields, including sociology [2,3], biology [4,5,6], and computer science [7,8], with specific uses in areas such as social media [9], healthcare [10], the web [11,12], and path searches [13,14]. A cluster, also referred to as a community, is a set of vertices that are more densely connected to each other than to the rest of the network. The community-based graph clustering problem involves partitioning the vertex set V of a graph into k non-empty subsets, with many edges within each cluster and relatively few edges between clusters. Successful clustering produces clusters with dense internal connections and sparse links between different clusters [15,17]. A visual representation of a network with this type of cluster structure is shown in Fig. 1. It is important to note that this paper focuses on clustering undirected unweighted graphs without self-loops and multiple edges, and we assume that vertices are assigned to non-overlapping clusters.

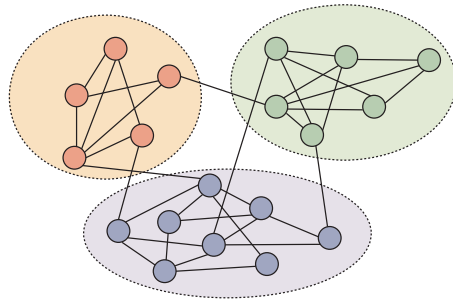


Fig. 1 A schematic representation of a network with cluster structure. In this network, there are three clusters of densely connected vertices (indicated by solid circles), which are represented by yellow, purple, and green dashed circles. The density of connections between these clusters is much lower

Unlike the common Euclidean space, graphs do not exist in the form of coordinates, and the distance between two nodes cannot be directly measured. Consequently, traditional clustering algorithms based on Euclidean space, such as K-means, are not applicable to graph clustering problems [16,17]. The methods for addressing graph clustering problems can be mainly categorized into five types: (1) spectral algorithms, which utilize the spectral properties of graphs to detect clusters [18,19]; (2) statistical inference-based [22] methods, such as Markov [20] and Bayesian ap-

proaches [21]; (3) dynamics-based methods, which involve running dynamic processes on the network to identify clusters, such as diffusion [23], spin dynamics [24, 25] and synchronization [26]; (4) divisive clustering algorithms, a class of top-down hierarchical methods that recursively partition the graph into clusters [32, 27, 28]; (5) optimization-based methods, where the clustering result is obtained by finding the extreme value of a function in the possible clustering space, such as maximizing modularity [27] (optimizing the modularity quality function) or maximizing similarity [31]. For a comprehensive and detailed overview of methods for solving graph clustering problems, readers are referred to [32, 15, 33].

Optimization-based methods are characterized by low computational cost and high accuracy. The maximization of the modularity function [27] is one of the most popular approaches for community detection, with the Louvain method designed by Blondel et al. [34] being the most well-known and effective modularity maximization technique. Although these methods offer advantages such as short computation time and the ability to operate without requiring the number of clusters as input parameter [17], they also have drawbacks, including the limitations of observed clusters [35], the resolution limit problem [36, 39] and the degeneracy problem [36, 45]. Consequently, many researchers have explored alternatives that do not rely on modularity maximization to address graph clustering problems, such as those found in [40, 41, 42]. Miasnikof et al. [17] were the first to extend the distance minimization of the binary quadratic formulas of Fan and Pardalos [31] to the general case of graph clustering problems. They employed the Jaccard distance to reflect connectivity and used a Boltzmann machine heuristic to solve the resulting model, which is presented below

$$\begin{aligned}
& \min_x \sum_i \sum_{j>i} \sum_k x_{ik} x_{jk} d_{ij} \\
& \text{s.t.} \sum_k x_{ik} = 1, \forall i, \\
& x_{ik} \in \{0, 1\}, \forall i, k.
\end{aligned} \tag{1}$$

Here x_{ik} is a binary variable that takes the value of 1 if the vertex i is assigned to the cluster k , and d_{ij} represents the Jaccard distance between i and j . Note that (1) is essentially a binary programming problem with semi-assignment constraints. Inspired by the approach in [44] to solve hypergraph matching problems, in this paper, we consider a general class of graph clustering problems (see (2)), and propose an efficient approach to solve it.

The contributions of this paper are as follows: (1) We first summarize several graph clustering models that can be uniformly formulated as semi-assignment problems with objective functions that have block properties. (2) For this class of problem, we equivalently reformulate them as sparse-constrained optimization problems. (3)

We apply a quadratic penalty method to the relaxation problem, and for the nonlinear quadratic penalty subproblem with simple box constraints, we employ a projected gradient method based on the active set. The special structure of this class of problems allows for the acceleration of the computation in this method. (4) Extensive numerical results indicate that, for synthetic or real-world graphs, this algorithm identifies more accurate clusters at a faster speed, especially in large-scale problems.

The remainder of this paper is organized as follows. In Sect. 2, we propose the semi-assignment optimization model for graph clustering and discuss its properties. In Sect. 3, we investigate the continuous relaxation problem and apply the fast quadratical penalty method to solve it. In Sect. 4, we present extensive numerical results to verify the efficacy of the proposed method. Final conclusions are given in Sect. 5.

2 Semi-assignment optimization model for graph clustering

In this section, we will establish the mathematical model for graph clustering, which can be cased as a semi-assignment optimization problem.

2.1 Optimization model based on semi-assignment constraints

To that end, we consider a graph $G = (V(G), E(G))$, where $V(G) = \{1, 2, \dots, n\}$ is a nonempty set of vertices and $E(G) = \{(i, j) \mid i, j = 1, \dots, n, i \text{ and } j \text{ is connected}\}$ is a set of edges. Let the set of all clusters be $\mathbb{C} = \{C_1, C_2, \dots, C_K\}$, where K is the number of clusters. We denote the total number of edges (or vertices) by $|E(G)|$ (or $|V(G)| = n$), and the number of vertices in the cluster i by $n^{(i)}$.

Roughly speaking, graph clustering involves dividing the vertices of a graph into several subsets of densely connected vertices, where vertices within the same subset have more common connections than those in different subsets. Mathematically speaking, let x_{ik} denote whether vertex i is assigned to cluster k , and x_{ik} is one if yes and zero otherwise. The essential aim of graph clustering is to assign each vertex a cluster such that some measures of the clustering is minimized. That is,

$$\begin{aligned} & \min_x f(x) \\ & s.t. \quad \sum_{k=1}^K x_{ik} = 1, \quad i = 1, \dots, n, \\ & \quad \quad x_{ik} \in \{0, 1\}, \quad i = 1, \dots, n, \quad k = 1, \dots, K, \end{aligned} \quad (2)$$

where x_{ik} is represented in the same way as in (1). Note that the constraint $\sum_k x_{ik} = 1$, $x_{ik} \in \{0, 1\}$, $\forall k$, describes the semi-assignment constraint [38]. Therefore, (2) is a semi-assignment optimization problem.

Here, $f(x)$ is a certain criterion to measure the qualification of graph clustering. Various choices of f can be used, such as [41, 17]. In this paper, we consider the following form of objective function in [17],

$$f(x) = \sum_i \sum_{j>i} \sum_k x_{ik} x_{jk} d_{ij},$$

where d_{ij} represents the distance between the vertex i and j . Below we mainly consider the following three choices of distances which are Burt's distance [48, 51, 52], Jaccard distance [49, 51, 52] and Otsuka-Ochiai distance [55, 51, 52]. As will be shown below, this objective function exhibits block properties.

To conclude this subsection, we would like to mention that there are also other criteria for f . For example, [41] focuses on maximizing the mean intra-cluster density while introducing a penalty function $P_k(M)$ to discourage clusters that are too large or too small. The penalty functions can be defined as $P_k(M) = \max\{0, \sum_i x_{ik}\}$ or $P_k(M) = (\sum_i x_{ik} - M)^2$, where M is a parameter. Then, the objective function becomes:

$$f(x) = - \sum_{k=1}^{|\mathcal{C}|} \left[\sum_{i,j} \left(\frac{w_{i,j} x_{ik} x_{jk}}{0.5 \times n^{(k)}(n^{(k)} - 1)} - \lambda P_k(M) \right) \right],$$

where $w_{i,j}$ is the weight of the edge connecting vertex i and vertex j , and λ is a penalty coefficient. Unfortunately, this objective function does not exhibit block properties (Prop. 3) and is computationally challenging.

2.2 Different distance metrics

As mentioned above, graph clustering is defined as subsets of vertices that are considered similar to some extent. This similarity is manifested through the number of shared connections and is translated into a distance metric. Therefore, the distance measure we need is based on similarity rather than the shortest path distance. The following lists three types of distance that are often used as similarity measures in graph clustering problems.

Burt's distance D^B

The Burt distance [51, 52], borrowed from sociology [48], is defined as follows for the distance between the vertex i and j :

$$D_{ij}^B = \sqrt{\sum_{s \neq i,j} (A_{is} - A_{js})^2},$$

where $A = (A_{ij}) \in \mathbb{R}^{n \times n}$ is the adjacency matrix. For an unweighted graph, $A_{ij} = 1$ if $(i, j) \in E(G)$ and 0 otherwise. For a weighted graph, if $(i, j) \in E(G)$, A_{ij} is the weight of the edge between i and j ; otherwise, $A_{ij} = 0$. Then Burt's distance matrix is defined as $D^B = (D_{ij}^B) \in \mathbb{R}^{n \times n}$.

Jaccard distance D^J

The Jaccard distance [51, 52], originating from botany [49], is defined between the vertex i and j as follows:

$$D_{ij}^J = \begin{cases} 1 - \frac{|a_i \cap a_j|}{|a_i \cup a_j|}, & i \neq j, \\ 0, & i = j, \end{cases}$$

where a_i denotes the set of all vertices that share an edge with vertex i . The ratio $\frac{|a_i \cap a_j|}{|a_i \cup a_j|}$ represents the Jaccard similarity. The above applies to the case of an unweighted graph. For a weighted graph, we use the following expression:

$$D_{ij}^J = \begin{cases} 1 - \frac{\sum_{s=1}^n \min\{w_{is}, w_{js}\}}{\sum_{s=1}^n \max\{w_{is}, w_{js}\}}, & i \neq j, \\ 0, & i = j, \end{cases}$$

where w_{is} denotes the weight of the edge between the vertex i and the vertex s . Note that $D_{ij}^J \in [0, 1]$. Then Jaccard distance matrix is defined as $D^J = (D_{ij}^J) \in \mathbb{R}^{n \times n}$.

Otsuka-Ochiai distance D^O

The Otsuka-Ochiai distance [51, 52] originates from zoology [55]. In the case of unweighted graphs, Otsuka-Ochiai distance between the vertex i and j is defined as follows:

$$D_{ij}^O = 1 - \frac{|a_i \cap a_j|}{\sqrt{|a_i| \times |a_j|}} \in [0, 1],$$

where a_i is the same as that in the Jaccard distance. In the weighted case, we use the following expression:

$$D_{ij}^O = 1 - \frac{\sum_{s=1}^n \min\{w_{is}, w_{js}\}}{\sqrt{\sum_{s=1}^n w_{is} \times \sum_{s=1}^n w_{js}}} \in [0, 1],$$

where w_{is} denotes the weight of the edge between the vertex i and s . Then Otsuka-Ochiai distance matrix is defined as $D^O = (D_{ij}^O) \in \mathbb{R}^{n \times n}$.

The three $n \times n$ distance matrices (denoted as D^B , D^J and D^O respectively) satisfy Prop. 1.

Proposition 1 For the matrix D defined by D^B , D^J or D^O as above, it holds that $D_{ij} \geq 0$, $D_{ii} = 0$, $D_{ij} = D_{ji}$, $i = 1, \dots, n$, $j = 1, \dots, n$. In other words, D is nonnegative, symmetric and has zero diagonal elements.

2.3 Equivalent formulation of (2)

Based on Sect. 2.1 and Sect. 2.2, the graph clustering model we consider in this paper takes the following form

$$\begin{aligned} \min_x \quad & \sum_i \sum_{j>i} \sum_k x_{ik} x_{jk} d_{ij} \\ \text{s.t.} \quad & \sum_k x_{ik} = 1, \quad i = 1, \dots, n, \\ & x_{ik} \in \{0, 1\}, \quad i = 1, \dots, n, \quad k = 1, \dots, K. \end{aligned} \quad (3)$$

Denote $\mathbf{x} = (\mathbf{x}_1^\top, \mathbf{x}_2^\top, \dots, \mathbf{x}_n^\top)^\top \in \mathbb{R}^{nK}$, $\mathbf{x}_i^\top = (x_{i1}, x_{i2}, \dots, x_{iK}) \in \mathbb{R}^K$. Then the sum of distances generated by the vertex i and j can be expressed as the following equation

$$\sum_k x_{ik} x_{jk} d_{ij} = \begin{bmatrix} x_{i1} & x_{i2} & \dots & x_{iK} \end{bmatrix} \begin{bmatrix} d_{ij} & 0 & \dots & 0 \\ 0 & d_{ij} & \dots & 0 \\ \vdots & \vdots & \ddots & \vdots \\ 0 & 0 & \dots & d_{ij} \end{bmatrix} \begin{bmatrix} x_{j1} \\ x_{j2} \\ \vdots \\ x_{jK} \end{bmatrix} = \mathbf{x}_i^\top (d_{ij} I_k) \mathbf{x}_j, \quad (4)$$

where $I_k \in \mathbb{R}^{K \times K}$ is an identity matrix. Let $\bar{\Delta}_{ij} = d_{ij} I_k \in \mathbb{R}^{K \times K}$ and $\Delta = D \otimes I_k \in \mathbb{R}^{nK \times nK}$. Then the objective function of (3) can be written as

$$\sum_i \sum_{j>i} \sum_k x_{ik} x_{jk} d_{ij} = \frac{1}{2} \begin{bmatrix} \mathbf{x}_1^\top & \mathbf{x}_2^\top & \dots & \mathbf{x}_n^\top \end{bmatrix} (D \otimes I_k) \begin{bmatrix} \mathbf{x}_1 \\ \mathbf{x}_2 \\ \vdots \\ \mathbf{x}_n \end{bmatrix} = \frac{1}{2} \mathbf{x}^\top \Delta \mathbf{x}. \quad (5)$$

Hence, (3) can be written in the following equivalent form

$$\begin{aligned} \min_{\mathbf{x}} \quad & f(\mathbf{x}) := \frac{1}{2} \mathbf{x}^\top \Delta \mathbf{x} \\ \text{s.t.} \quad & \mathbf{x}_i^\top \mathbf{1}_k = 1, \quad i = 1, \dots, n, \\ & \mathbf{x} \in \{0, 1\}^{nK}, \end{aligned} \quad (6)$$

where $\mathbf{1}_k = [1, 1, \dots, 1]^\top \in \mathbb{R}^K$. (6) can also be written in the following equivalent form:

$$\begin{aligned} \min_{\mathbf{x} \in \mathbb{R}^{nK}} \quad & f(\mathbf{x}) \\ \text{s.t.} \quad & \mathbf{x}_i^\top \mathbf{1}_k = 1, \quad i = 1, \dots, n, \\ & \mathbf{x} \geq 0, \\ & \|\mathbf{x}\|_0 \leq n. \end{aligned} \quad (7)$$

In (7), we remove the last constraint $\mathbf{x} \in \{0, 1\}^{nK}$ of (6), and add two constraints, $\|\mathbf{x}\|_0 \leq n$ and $\mathbf{x} \geq 0$. Due to the constraint $\mathbf{x}_i^\top \mathbf{1}_k = 1$, $i = 1, \dots, n$, we know that $\|\mathbf{x}\|_0 \geq n$. Additionally, because of the last constraint $\|\mathbf{x}\|_0 \leq n$, we have $\|\mathbf{x}\|_0 = n$.

The following result is obvious due to the definition of Δ .

Proposition 2 Recall $\Delta = D \otimes I_k$. It holds that $\Delta_{ii} = 0$, $\Delta_{ij} = \Delta_{ji}$, $i = 1, 2, \dots, nK$, $j = 1, 2, \dots, nK$. In other words, Δ is nonnegative, symmetric and has zero diagonal elements.

To present the property of $f(\mathbf{x})$, let an index $i_0 \in \{1, 2, \dots, n\}$ and the set $I^{-i_0} = \{1, 2, \dots, i_0 - 1, i_0 + 1, \dots, n\}$. We can rewrite $f(\mathbf{x})$ in (6) as:

$$\begin{aligned} f(\mathbf{x}) &= \frac{1}{2} \sum_{i=1}^n \sum_{j \neq i} \mathbf{x}_i^\top \bar{\Delta}_{ij} \mathbf{x}_j \\ &= \frac{1}{2} \left(2\mathbf{x}_{i_0}^\top \sum_{j \neq i_0} \bar{\Delta}_{i_0 j} \mathbf{x}_j + \sum_{i \in I^{-i_0}} \sum_{j \neq i, j \in I^{-i_0}} \mathbf{x}_i^\top \bar{\Delta}_{ij} \mathbf{x}_j \right) \\ &= \mathbf{x}_{i_0}^\top \sum_{j \neq i_0} \bar{\Delta}_{i_0 j} \mathbf{x}_j + \frac{1}{2} \sum_{i \in I^{-i_0}} \sum_{j \neq i, j \in I^{-i_0}} \mathbf{x}_i^\top \bar{\Delta}_{ij} \mathbf{x}_j \\ &:= f^{(i_0)}(\mathbf{x}) + f^{(-i_0)}(\mathbf{x}). \end{aligned} \quad (8)$$

We have the following result.

Proposition 3 $f^{(i)}(\mathbf{x}) = \mathbf{x}_i^\top \nabla_{\mathbf{x}_i} f(\mathbf{x})$, $i \in \{1, 2, \dots, n\}$.

Proof. According to (4) and (5), we know that

$$f(\mathbf{x}) = \frac{1}{2} \mathbf{x}^\top \Delta \mathbf{x} = \sum_i \sum_{j > i} \mathbf{x}_i^\top \bar{\Delta}_{ij} \mathbf{x}_j.$$

Then $\nabla_{\mathbf{x}_i} f(\mathbf{x}) = \sum_{j \neq i} \bar{\Delta}_{ij} \mathbf{x}_j$. Due to (8), we have

$$f^{(i_0)}(\mathbf{x}) = \mathbf{x}_{i_0}^\top \sum_{j \neq i_0} \bar{\Delta}_{i_0 j} \mathbf{x}_j = \mathbf{x}_{i_0}^\top \nabla_{\mathbf{x}_{i_0}} f(\mathbf{x}).$$

Then for every index $i \in \{1, 2, \dots, n\}$, $f^{(i)}(\mathbf{x}) = \mathbf{x}_i^\top \nabla_{\mathbf{x}_i} f(\mathbf{x})$. \square

Remark 1 The above proposition demonstrates that for each block \mathbf{x}_i , $f(\mathbf{x})$ is basically a linear function with respect to \mathbf{x}_i . This is a key property which will be further explored in the subsequent of the paper.

3 Continuous relaxation of (7) and a fast algorithm

In this section, we relax the sparse constraint problem (7) to a continuous problem and propose a fast quadratic penalty algorithm to solve the relaxation problem.

3.1 Relaxation problem

Both (6) and (7) are essentially a discrete optimization problem, which is in general NP hard and therefore is extremely difficult to solve. A popular way to deal with (6) or (7) is to relax the discrete constraint and consider solving the relaxed continuous problem. By removing the last constraint in (7), we obtain the following relaxation problem

$$\begin{aligned} \min_{\mathbf{x} \in \mathbb{R}^{nK}} \quad & f(\mathbf{x}) \\ \text{s.t.} \quad & \mathbf{x}_i^\top \mathbf{1}_k = 1, \quad i = 1, \dots, n, \\ & \mathbf{x} \geq 0. \end{aligned} \quad (9)$$

(9) is a continuous problem with simplex constraints. Due to Prop. 3, the following result holds by Thm. 1 in [44], which address the relation between (7) and the relaxation problem (9).

Theorem 1 *There exists a global minimum \mathbf{x}^* of the problem (9) such that $\|\mathbf{x}^*\|_0 = n$, and the global minimizer $\mathbf{x}^* \in \mathbb{R}^{nK}$ is also a global minimizer of the problem (7).*

Based on Thm. 1, starting from any global minimizer of problem (9), we can eventually find a point \mathbf{x}^* that is a global minimizer of both (9) and (7). Therefore, we can find a global minimizer of (7) using the approach described in Alg. 1 below.

Algorithm 1 The procedure of finding a global minimizer of (7)

- 1: **Input:** a global minimizer of (9): $\mathbf{y}^0 = ((\mathbf{y}_1^0)^\top, (\mathbf{y}_2^0)^\top, \dots, (\mathbf{y}_n^0)^\top)^\top \in \mathbb{R}^{nK}$. Let $\mathbf{x} = ((\mathbf{x}_1)^\top, (\mathbf{x}_2)^\top, \dots, (\mathbf{x}_n)^\top)^\top = \mathbf{0} \in \mathbb{R}^{nK}$;
 - 2: **for** $i = 1 : n$ **do**
 - 3: For i -th block \mathbf{y}_i^0 of \mathbf{y} , we find an index p^i which $(\mathbf{y}_i^0)_{p^i} \geq (\mathbf{y}_i^0)_q, q = 1, 2, \dots, K$.
 - 4: Let $(\mathbf{x}_i)_{p^i} = 1$.
 - 5: **end for**
 - 6: **Output:** $\mathbf{x} = ((\mathbf{x}_1)^\top, (\mathbf{x}_2)^\top, \dots, (\mathbf{x}_n)^\top)^\top \in \mathbb{R}^{nK}$, which is a global minimizer of (7).
-

3.2 Quadratic penalty method

To solve the continuous relaxation problem (9), various optimization methods can be used. It has been verified in [43,44] that the quadratic penalty method is highly efficient in solving such kind of problem. Therefore, in this paper, we continue to apply the quadratic penalty method to solve (9). The idea of this method is as follows. Due to the result in Thm. 1, there is no need to solve (9) to get an accurate global minimizer. All we need is to identify the support set of the global minimizer of (9) so

that we can use Alg. 1 to obtain a global minimizer of (7). Therefore, we can penalize the equality constraint and in each iteration, we solve the quadratic penalty problem

$$\min_{0 \leq \mathbf{x} \leq M} g^l(\mathbf{x}) := f(\mathbf{x}) + \frac{\theta_l}{2} \sum_{i=1}^n (\mathbf{x}_i^\top \mathbf{1}_k - 1)^2, \quad (10)$$

where $M \geq 1$ is a given value and the upper bound $\mathbf{x} \leq M$ is added to make sure that the penalty problem is well-defined. Details of the quadratic penalty method are given in Alg. 2.

Algorithm 2 Quadratic penalty method

```

1: Input: an initial point  $\mathbf{x}^0$ , a parameter  $\theta_0 > 0$ ,  $l = 0$ ;
2: for  $l$  do
3:   Solve (10) to get a  $\mathbf{x}^l$ .
4:   if the termination rule is not satisfied then
5:     Choose parameter  $\theta_{l+1} \geq \theta_l$ ;  $l = l + 1$ ;
6:   else
7:     break;
8:   end if
9: end for
10: Apply Alg. 1 to  $\mathbf{x}^l$  to get a global minimizer of (7).

```

Theorem 2 ([56,57]) *Let $\{\mathbf{x}^l\}$ be the sequence generated by Alg. 2, and assume that \mathbf{x}^l is a global minimizer of (10). Let $\lim_{l \rightarrow \infty} \theta_l = +\infty$. Then any accumulation point of this generated sequence is a global minimum of (9).*

Thm. 2 addresses the convergence of the quadratic penalty method. A detailed proof can be found in [56,57].

Assumption 1 *Let $\{\mathbf{x}^l\}$ be the sequence generated by Alg. 2, with $\lim_{l \rightarrow \infty} \theta_l = +\infty$. Here, l is a positive integer. Suppose $\lim_{l \rightarrow \infty} \mathbf{x}^l = \mathbf{z}$, and \mathbf{z} is a global minimizer of (9).*

Define the support set at \mathbf{x} by $\Gamma(\mathbf{x}) := \{j : \mathbf{x}_j > 0\}$. Based on Thm. 3 and Thm. 4 in [44], the following result holds.

Theorem 3 *Under Assump. 1, there exists a global minimizer \mathbf{z}^* of (7) such that for l sufficiently large, it holds that $\Gamma(\mathbf{x}^l) = \Gamma(\mathbf{z}^*)$.*

Thm. 3 shows that under Assump. 1, the support set of the global minimizer for the original problem (7) can be precisely recovered when the number of iterations is sufficiently large.

Inspired by [44], we employ a projected gradient method based on the active set to solve the subproblem (10), as detailed in [44] Alg. 3. Our primary goal is to identify

the support set of the global minimizer of (7), rather than its magnitude. Therefore, the projected gradient method is applied to the nonlinear problem (10) with simple box constraints.

4 Numerical Results

In this section, we evaluate the performance of our algorithm on different data sets. We compare the solution quality of our algorithm (QP-GC) with the leading commercial solver Gurobi [58] for (3) and the Boltzmann machine (BM) from the latest research [17]. Additionally, we conduct case studies on two real-world graphs. We implement the Boltzmann machine by ourselves, since the original code is not available. Our algorithm, the Boltzmann machine and Gurobi run on a 4-core/8-thread machine. All experiments are written in MATLAB R2022a¹ running in Windows 10 on an Intel(R) Core(TM) i7-1065G7 CPU at 1.30 GHZ with 16.0 GB of RAM, and all graphs are generated using Python 3.8².

4.1 Evaluation of clustering quality

To start with, we introduce some measures to evaluate the clustering quality. We use the comparison of intra-cluster density, inter-cluster density, and overall density as metrics to evaluate clustering quality. It is demonstrated in [45] and [46] that the evaluation of the quality of the cluster using these metrics is far superior to the most popular graph cluster quality function, i.e., modularity [47].

The number of edges connecting vertices within cluster i is denoted as $|E_{ii}|$, and the number of edges connecting a vertex in cluster i to a vertex in cluster j is denoted as $|E_{ij}|$. The overall density is defined by

$$\kappa = \frac{|E(G)|}{0.5 \times n(n-1)}.$$

For a cluster i , the intra-cluster density is given by

$$\kappa_{intra}^{(i)} = \frac{|E_{ii}|}{0.5 \times n^{(i)}(n^{(i)} - 1)}.$$

For a cluster i and a cluster j , $i \neq j$, the inter-cluster density is given by

$$\kappa_{inter}^{(ij)} = \frac{|E_{ij}|}{n^{(i)} \times n^{(j)}}.$$

¹ <https://ww2.mathworks.cn>

² <https://www.python.org/downloads/>

For a graph clustered into K clusters, the mean intra-cluster density and the mean inter-cluster density are given respectively by

$$\bar{\kappa}_{intra} = \frac{1}{K} \sum_{i=1}^K \kappa_{intra}^{(i)}, \quad \bar{\kappa}_{inter} = \frac{1}{0.5 \times K(K-1)} \sum_{i=1}^K \sum_{j=i+1}^K \kappa_{inter}^{(ij)}.$$

Using the quantities defined above, we can measure the quality of clustering. A high quality clustering groups vertices into clusters such that, on average, the links between vertices within these clusters are denser than the links between vertices in different clusters [45, 46]. Therefore, a high quality clustering should satisfy the following inequality

$$\bar{\kappa}_{inter} < \kappa < \bar{\kappa}_{intra}. \quad (11)$$

For the choice of distance, considering factors such as wide applicability, computational complexity, and interpretability, we take the Jaccard distance as the measurement to report our result. Furthermore, it is both demonstrate in [51, 52] that the Jaccard distance is the most suitable distance metric for graph clustering.

4.2 Synthetic graphs

In this part, we perform experiments on nine different synthetic graphs, generated using two different models: the Planted Partition Model (PPM) [30] and the Stochastic Block Model (SBM) [37]. These graphs have known classification properties, as detailed in Tab. 1. The graphs are generated using the NetworkX Python library [29]. The clustering process becomes more complicated as intra-cluster edge probability decreases, inter-cluster edge probability increases, and cluster sizes vary. An increase in the number of graph vertices also adds to the computational difficulty.

It is worth noting that the mean intra-cluster density $\bar{\kappa}_{intra}$ (or the mean inter-cluster density $\bar{\kappa}_{inter}$) is an empirical estimate of the intra-cluster edge probability P_{intra} (or the inter-cluster edge probability P_{inter}) in the generated models, as has been demonstrated by [17]. Therefore, the closer $\bar{\kappa}_{intra}$ (or $\bar{\kappa}_{inter}$) calculated from the clustering obtained by a given method is to P_{intra} (or P_{inter}) of the generation model, the higher the quality of the solution generated by that method. This also indicates that the clustering performance of the method is better.

4.2.1 Performance for QP-GC

We first test on three PPM graph models with 250 vertices, each containing five clusters with 50 vertices per cluster. Secondly, we test on six SBM graph models with 3000 vertices. Each graph contains 30 clusters, with cluster sizes ranging from 25 to 200 vertices. For each intra-cluster edge probability, two different inter-cluster edge

Table 1 Details of nine synthetic graphs.

Model type	Graph name	P_{intra}	P_{inter}	K	n	Cluster sizes
PPM	G1_PPM	0.9	0.1	5	250	50
PPM	G2_PPM	0.85	0.15	5	250	50
PPM	G3_PPM	0.8	0.2	5	250	50
SBM	G1_SBM	0.9	0.05	30	3000	[25,200]
SBM	G2_SBM	0.9	0.1	30	3000	[25,200]
SBM	G3_SBM	0.85	0.05	30	3000	[25,200]
SBM	G4_SBM	0.85	0.1	30	3000	[25,200]
SBM	G5_SBM	0.8	0.05	30	3000	[25,200]
SBM	G6_SBM	0.8	0.1	30	3000	[25,200]

probabilities are used to create the graphs. These graphs are generated using the following intra-cluster/inter-cluster edge probabilities ($P_{\text{intra}}/P_{\text{inter}}$) as shown in Tab. 1. The variability in cluster sizes, along with the large number of vertices, adds the complexity to the clustering problem.

The proposed QP-GC method for solving graph clustering problems is tailored to the problem (3). This is due to the objective function and its gradient given by $\nabla_{\mathbf{x}_i} f(\mathbf{x}) = \sum_{j \neq i} \bar{\Delta}_{ij} \mathbf{x}_j$. Additionally, (3) involves only a single vector variable $\mathbf{x} > 0$ and n linear equality constraints, all of which are linear. These characteristics ensure that the computational process runs efficiently.

The parameters for our method are set as follows. In Alg. 2, we set the initial point \mathbf{x}^0 as a random matrix. Update θ_l as

$$\theta_{l+1} = \begin{cases} 3\theta_l, & \text{if } \|h^l\| > 0.01 \text{ and } \theta_l < \bar{\theta}, \\ \theta_l, & \text{otherwise,} \end{cases}$$

where $h^l = ((\mathbf{x}_1^l)^\top \mathbf{1} - 1, \dots, (\mathbf{x}_n^l)^\top \mathbf{1} - 1)$. For the experiments on the PPM model, we set $\bar{\theta} = 10^5$ and $\theta_0 = 10$, while for the experiments on the SBM model, we set $\bar{\theta} = 10^{10}$ and $\theta_0 = 2500$. Each \mathbf{x}^l returned is projected onto a binary assignment matrix using Alg. 1. For the experiments on the small-scale PPM model, we set $\varepsilon = 0.0009$, while for the large-scale SBM model experiments, we set $\varepsilon = 2 \times 10^{-8}$.

Results on PPM graph models

We test on three PPM models. In Tab. 2, $\varepsilon_{\text{intra}}$ (or $\varepsilon_{\text{inter}}$) represents the absolute value of the difference between $\bar{\kappa}_{\text{intra}}$ (or $\bar{\kappa}_{\text{inter}}$) computed by QP-GC and P_{intra} (or P_{inter}) in the graph. We say that the smaller its value, the more accurate the clustering result, especially with regard to $\varepsilon_{\text{intra}}$. We also report the CPU time and the number of iterations C_{iter} for QP-GC.

To provide a more intuitive demonstration of QP-GC, we visualized the above three graphs before and after clustering, as shown in Fig. 2. The visualizations of

Table 2 Numerical results of QP-GC for three PPM models with $n = 250$ and $K = 5$.

Graph name	Graph characteristics			QP-GC					
	P_{intra}	P_{inter}	κ	$\bar{\kappa}_{intra}$	$\bar{\kappa}_{inter}$	ϵ_{intra}	ϵ_{inter}	times(s)	C_{iter}
G1_PPM	0.9	0.1	0.26	0.90	0.10	0	0	0.6	230
G2_PPM	0.85	0.15	0.29	0.85	0.15	0	0	0.8	320
G3_PPM	0.8	0.2	0.32	0.80	0.20	0	0	0.9	430

the three PPM graphs are shown in the left column of Fig. 2. The right column of Fig. 2 show the graph after clustering with QP-GC, where the graph is divided into five clusters, with each color representing a different cluster. Fig. 2 illustrates that our method accurately partitions three graphs into five clusters, demonstrating high-quality clustering. This visual representation is sufficient to show the effectiveness of QP-GC.

Results on SBM graph models

We test on six SBM models. In Tab. 3, ϵ_{intra} (or ϵ_{inter}) is defined in the same way as in Tab. 2. Additionally, we also list the CPU time and the number of iterations for our method. Note that the experiments are conducted on SBM models with 3000 nodes, 30 clusters, and the number of nodes in each cluster randomly chosen from the range [25, 200]. Due to the complexity of this scenario, visualizations, as in Fig. 2, are not intuitive. However, ϵ_{intra} (or ϵ_{inter}) is sufficient to demonstrate the clustering performance. As shown in Tab. 3, the more complex the graph, the greater the number of iterations required and the longer the CPU time.

Table 3 Numerical results of QP-GC for six SBM models with $n = 3000$ and $K = 30$.

Graph name	Graph characteristics			QP-GC					
	P_{intra}	P_{inter}	κ	$\bar{\kappa}_{intra}$	$\bar{\kappa}_{inter}$	ϵ_{intra}	ϵ_{inter}	times(mm:ss)	C_{iter}
G1_SBM	0.90	0.05	0.09	0.78	0.06	0.12	0.01	17:07	2930
G2_SBM	0.90	0.10	0.14	0.73	0.12	0.17	0.02	43:17	6000
G3_SBM	0.85	0.05	0.09	0.73	0.06	0.12	0.01	27:26	4560
G4_SBM	0.85	0.10	0.13	0.72	0.11	0.13	0.01	43:39	6630
G5_SBM	0.80	0.05	0.08	0.65	0.06	0.15	0.01	30:16	5000
G6_SBM	0.80	0.10	0.13	0.66	0.11	0.14	0.01	44:33	6750

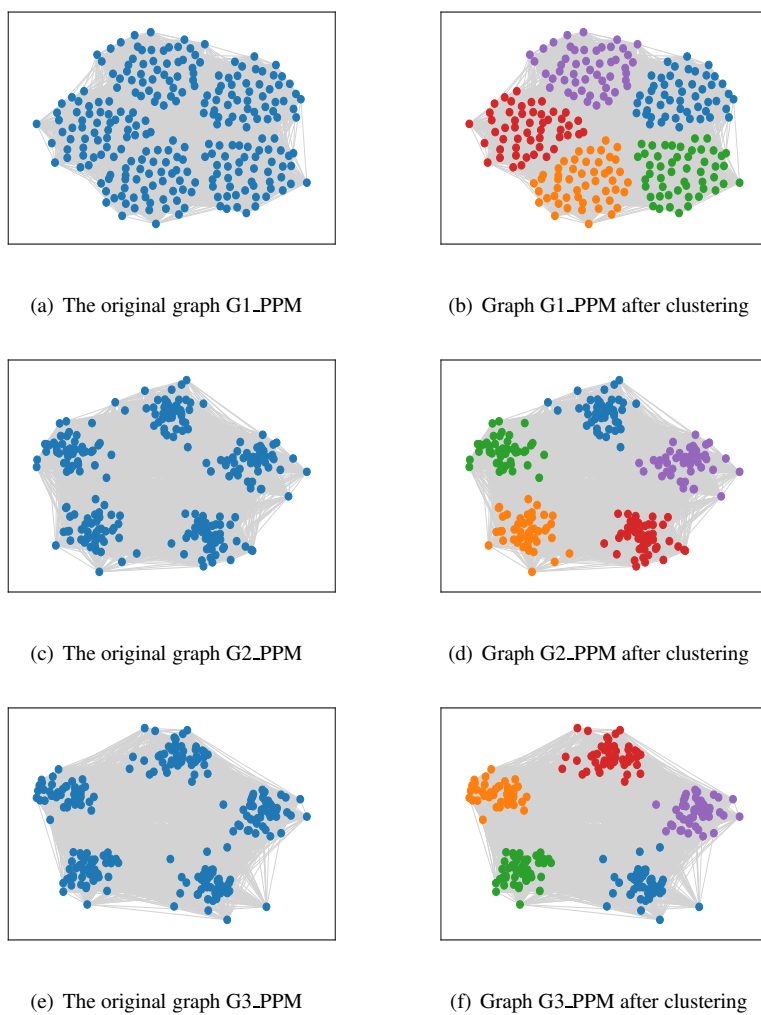


Fig. 2 A visual representation of three PPM graph models after clustering with our method

4.2.2 Comparison with other algorithms

Results on PPM graph models

The numerical results are presented in Tab. 4. We compare QP-GC with Gurobi and BM in terms of ϵ_{intra} , ϵ_{inter} , and CPU time. From Tab. 5, we can observe that all three solutions produce the same results, and all satisfy (11). In all three cases (G1_PPM, G2_PPM and G3_PPM), they perfectly recover the generation model. We would like

to emphasize that in this example, it can be noticed that under the same conditions, our method achieves accurate clustering results in a shorter CPU time.

Table 4 Numerical results of three methods for three PPM models with $n = 250$ and $K = 5$.

Graph name	Graph characteristics			QP-GC		Gurobi		BM	
	P_{intra}	P_{inter}	κ	$\bar{\kappa}_{intra}$	$\bar{\kappa}_{inter}$	$\bar{\kappa}_{intra}$	$\bar{\kappa}_{inter}$	$\bar{\kappa}_{intra}$	$\bar{\kappa}_{inter}$
G1_PPM	0.90	0.10	0.26	0.90	0.10	0.90	0.10	0.90	0.10
G2_PPM	0.85	0.15	0.29	0.85	0.15	0.85	0.15	0.85	0.15
G3_PPM	0.80	0.20	0.32	0.80	0.20	0.80	0.20	0.80	0.20

Table 5 Comparison of some clustering metrics on PPM models.

Methods	G1_PPM			G2_PPM			G3_PPM		
	ϵ_{intra}	ϵ_{inter}	times(s)	ϵ_{intra}	ϵ_{inter}	times(s)	ϵ_{intra}	ϵ_{inter}	times(s)
QP-GC	0	0	0.6	0	0	0.8	0	0	0.9
Gurobi	0	0	3.2	0	0	3.1	0	0	3.1
BM	0	0	3.5	0	0	3.6	0	0	3.7

Results on SBM graph models

The characteristics of the graphs and the numerical results are reported in Tab. 6. Similarly, we compare QP-GC with Gurobi and BM in terms of ϵ_{intra} , ϵ_{inter} , and CPU time. Using the CPU time required by QP-GC to obtain the results as a benchmark, we compare the clustering quality returned by the three methods within that time period. Based on the results in Tab. 6 and Tab. 7, we summarize the following two observations:

- It is observed that the results obtained by QP-GC and BM both satisfy the inequality (11). However, Gurobi fails to return meaningful results under the same conditions, and the inequality does not hold (indicated by underline in Tab. 6).
- We notice significant differences in the results among the solvers. As shown in Tab. 7, within the same CPU time, our method achieves better clustering quality for this type of model compared to the solution returned by BM. In the case of larger and more complex SBM graphs, our method provides both faster and more reliable results for these models.

Table 6 Numerical results of three methods for six SBM models with $n = 3000$ and $K = 30$.

Graph name	Graph characteristics			QP-GC		Gurobi		BM	
	P_{intra}	P_{inter}	κ	$\bar{\kappa}_{intra}$	$\bar{\kappa}_{inter}$	$\bar{\kappa}_{intra}$	$\bar{\kappa}_{inter}$	$\bar{\kappa}_{intra}$	$\bar{\kappa}_{inter}$
G1_SBM	0.90	0.05	0.09	0.78	0.06	<u>0.33</u>	<u>0.32</u>	0.10	0.09
G2_SBM	0.90	0.10	0.14	0.72	0.12	<u>0.32</u>	<u>0.32</u>	0.15	0.14
G3_SBM	0.85	0.05	0.09	0.73	0.06	<u>0.30</u>	<u>0.29</u>	0.10	0.08
G4_SBM	0.85	0.10	0.13	0.72	0.11	<u>0.34</u>	<u>0.34</u>	0.14	0.13
G5_SBM	0.80	0.05	0.08	0.65	0.06	<u>0.26</u>	<u>0.26</u>	0.10	0.08
G6_SBM	0.80	0.10	0.13	0.66	0.11	<u>0.23</u>	<u>0.24</u>	0.14	0.13

Table 7 Comparison of some clustering metrics on SBM models.

Methods	G1_SBM (times 17:07)		G2_SBM (times 43:17)		G3_SBM (times 27:26)	
	ϵ_{intra}	ϵ_{inter}	ϵ_{intra}	ϵ_{inter}	ϵ_{intra}	ϵ_{inter}
QP-GC	0.12	0.01	0.17	0.02	0.12	0.01
Gurobi	0.57	0.27	0.58	0.22	0.55	0.24
BM	0.80	0.04	0.75	0.04	0.75	0.03

Methods	G4_SBM (times 43:39)		G5_SBM (times 30:16)		G6_SBM (times 44:33)	
	ϵ_{intra}	ϵ_{inter}	ϵ_{intra}	ϵ_{inter}	ϵ_{intra}	ϵ_{inter}
QP-GC	0.13	0.01	0.15	0.01	0.14	0.01
Gurobi	0.51	0.24	0.54	0.21	0.57	0.14
BM	0.71	0.03	0.70	0.03	0.66	0.03

To clearly and intuitively demonstrate the superiority of our method, we represent P_{intra} and $\bar{\kappa}_{intra}$ from Tab. 6 using radar plots, as shown in Fig. 3(a), and similarly represent P_{inter} and $\bar{\kappa}_{inter}$ using radar plots, as shown in Fig. 3(b). From Fig. 3, we observe that, regardless of the SBM graph model, $\bar{\kappa}_{intra}$ and $\bar{\kappa}_{inter}$ produced by our method (represented by the blue line) are closer to the P_{intra} and P_{inter} of the graph model (represented by the red line).

4.3 Real-world graphs

Although synthetic networks provide a repeatable and controlled testing platform for our experiments, testing algorithms on real-world network data is also necessary, even if real-world graphs are often not the best benchmarks for assessing clustering quality. In this section, we select two representative real-world network datasets: *Zachary's*

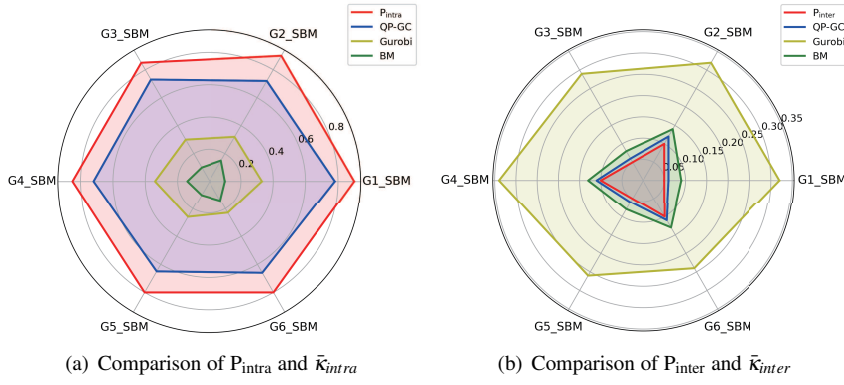


Fig. 3 The radar plot representation of P_{intra} (or P_{inter}) and $\bar{\kappa}_{intra}$ (or $\bar{\kappa}_{inter}$) in Tab. 6

Karate Club (Karate_club) [3] and the *United States College Football Division IA 2000 season* graph (US_football_2000) [3]. Both contain a known clustering structure. The graph data used in our experiments are available at <https://github.com/qinyuenlp/CommunityDetection/tree/main>. The characteristics of these graphs are shown in Tab. 8.

Table 8 Graph characteristics of two real-world graphs.

Graph name	Graph characteristics			
	$ V $	$ E $	κ	Clusters
Karate_club	34	78	0.14	2
US_football_2000	115	613	0.09	12

For experiments on real-world graphs, the following two points must be noted: (1) Real-world graphs are often instances of unknown underlying generative models with random noise. In many cases, modifying the clustering assignment of real-world graph vertices may result in higher intra-cluster density. This means that the true clustering results of the real-world graph vertices may not correspond to the clusters with the highest density. (2) When comparing the clustering results with the true clusters in real-world graphs, it is not sufficient to simply compare the cluster labels. Instead, the comparison should focus on the composition of the clusters. For instance, the cluster C_1 in the true clustering might not correspond to C_1 from the QP-GC clustering result, but it might fully correspond to C_2 from the QP-GC result. These two factors determine that we need to set evaluation criteria different from those used in the synthetic graph experiments.

For both of the following experiments, we use the same parameter settings. $\theta_0 = 20$ and the initial point S^0 is set as a random matrix. We set $\varepsilon = 10^{-5}$ in [44] Alg. 3.

For the termination condition, we set $\tau = 0.01$. Other parameters are the same as the PPM experiments.

4.3.1 Karate club study of Zachary

The real-world graph network data in this subsection comes from Zachary's famous study of the karate club [3]. The vertices of the graph represent the 34 members of the karate club, and the edges represent the social connections between the members. Here, we use the simplified unweighted version of the network. The club split into two factions due to internal conflict, and this division is reflected in the graph structure, as shown in Fig. 4(a). Note that in each subfigure of Fig. 4, nodes with the same color indicate that they belong to the same cluster. However, the same color across different subfigures does not convey any particular meaning.

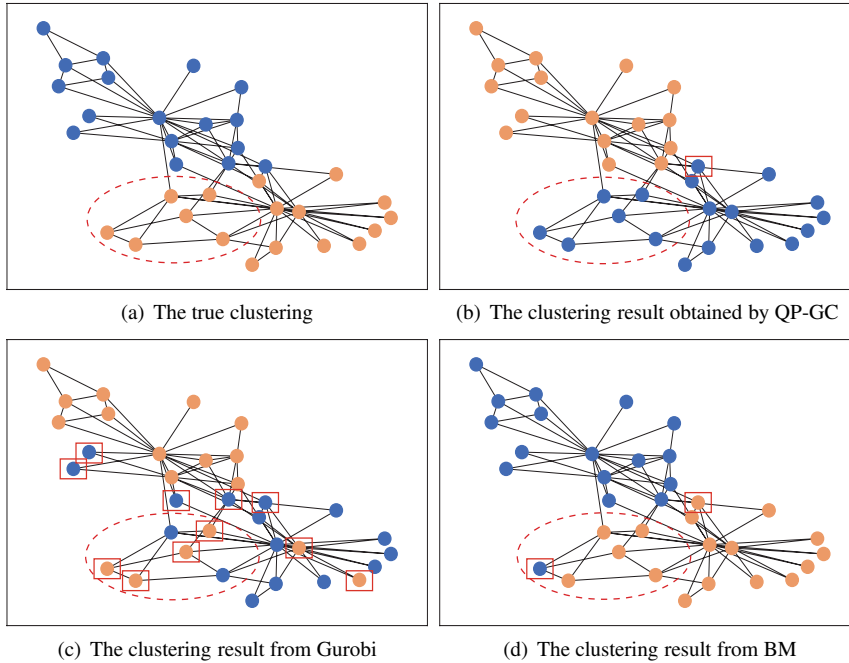


Fig. 4 The friendship network derived from Zachary's karate club, as described in this paper. Nodes of different colors represent membership in different factions. The red squares in the figure indicate the nodes of clustering error

We apply our method to this graph to identify the factions involved in the club's split. In addition, under the same CPU time (1 second), we compare the clustering results obtained using Gurobi and BM with those produced by our method. Both

Gurobi and BM have been shown to be effective for clustering in [17]. Since the graph has two cluster structures, we visualize the clustering, making the results visually clear, as shown in Fig. 4. We find that our QP-GC method misclassifies only one node, as shown in Fig. 4(b), while Gurobi misclassifies 11 nodes, as shown in Fig. 4(c), and BM misclassifies two nodes, as shown in Fig. 4(d). Thus, our method more accurately restores the clustering. Specifically, we observe six nodes circled by the red dashed ellipse in Fig. 4. These six nodes are shown as belonging to the same cluster in Fig. 4(a), and in Fig. 4(b), they are classified into the same cluster by QP-GC. However, in Fig. 4(c) and Fig. 4(d), it is shown that these nodes are not grouped together.

4.3.2 US College Football Division IA 2000 season graph

This subsection uses the well-known United States College Football Division IA 2000 season graph [3], which represents the matchups between 115 college football teams during the regular season. The vertices in the graph represent the teams, labeled by their university names, and the edges indicate that the two connected teams have faced each other at least once during the regular season. These teams are divided into 12 conferences, with each conference containing approximately 8-12 teams. Teams within the same conference compete more frequently against each other than against teams from different conferences, resulting in more shared connections among teams in the same conference compared to those in different ones.

We also compared the clustering results of QP-GC with Gurobi and BM when running for the same CPU time (1 second). The graph consists of 12 clusters, as shown in Fig. 5, where each circle represents a cluster. We assign 12 different colors to these circles. QP-GC misclassifies 12 nodes, as shown in Fig. 5(b), while Gurobi misclassifies 60 nodes, as shown in Fig. 5(c) and BM misclassifies 17 nodes, as shown in Fig. 5(d). Therefore, our method more accurately recovers the clustering structure. Specifically, we observe the 11 nodes circled by the red dashed ellipse in Fig. 5. These 11 nodes originally belong to the same cluster (as shown in Fig. 5(a)). In Fig. 5(b), QP-GC classifies these 11 nodes into the same cluster, while in Fig. 5(c) and Fig. 5(d), it is clear that they are not grouped together.

The large number of clusters (12 cluster structures) makes Fig. 5 less intuitive and clear. To better compare the clustering results, and considering the two key factors mentioned earlier for experiments on real-world graphs, we also use the Jaccard similarity function $J_{C_j}^y$ to compare the compositions of the true clusters and the clusters identified by various methods.

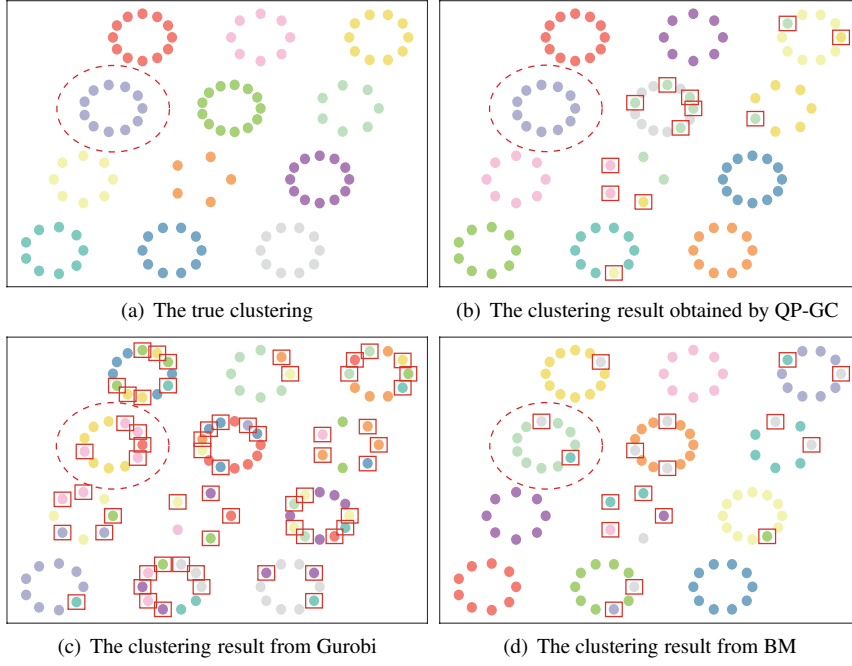


Fig. 5 A visualization of the US College Football Division IA 2000 season graph. Each circle represents nodes (teams) belonging to the same cluster, while red squares indicate misclassified nodes

This is expressed as

$$J_{C_j^\psi} = \max_{C_i^{true}} \left\{ \frac{|C_i^{true} \cap C_j^\psi|}{|C_i^{true} \cup C_j^\psi|} \right\},$$

where C_i^{true} represents the set of nodes in the i -th true cluster, and C_j^ψ denotes the set of nodes in the j -th cluster obtained by method ψ . We know $0 \leq J_{C_j^\psi} \leq 1$. The value produced by a perfect match between the j -th cluster identified by method ψ and its corresponding true cluster is $J_{C_j^\psi} = 1$, while a complete mismatch results in $J_{C_j^\psi} = 0$. We then have a set of $J_{C_j^\psi}$ defined as $\mathbb{J}^\psi = \{J_{C_j^\psi}, j = 1, \dots, k\}$. Let $\mathbb{J}_p^\psi = \{J_{C_j^\psi} : J_{C_j^\psi} = 1, j = 1, \dots, k\}$, we calculate $|\mathbb{J}_p^\psi|$. We also calculate the mean value $\bar{\mathbb{J}}^\psi$ of all elements in \mathbb{J}^ψ to provide an intuitive and effective comparison of the results, where a larger mean indicates better clustering performance. The comparison is listed in Tab. 9. These data show that our method achieves a better match to the true clusters for this class of optimization models.

To conclude, we find that our method demonstrates the ability to recover clusters not only in synthetic graphs but also in real-world graphs.

Table 9 Some reference values related to $J_{C_j^\psi}$ for comparison with true clusters.

Reference values	Method ψ		
	QP-GC	Gurobi	BM
$ \mathbb{J}_p^\psi $	6	0	2
$\bar{\mathbb{J}}^\psi$	0.83	0.34	0.77

5 Conclusion

In this paper, we considered a class of optimization models for graph clustering problems in a unified manner. We reformulated these models as sparse-constrained optimization problems and recovered the solutions of the original problem from the solutions of the relaxed problem without sparse constraints. A quadratic penalty method was applied to the relaxed problem. Our method QP-GC was compared with Gurobi and the Boltzmann machine. Through extensive numerical experiments, we found that, for both synthetic and real-world graphs, QP-GC not only outperformed the other methods in speed but also provided more accurate clustering results.

References

- Rossi R A, Jin D, Kim S et al (2020) On proximity and structural role-based embeddings in networks: Misconceptions, techniques, and applications. *Acm T Knowl Discov D* 14(5):1-37. <https://doi.org/10.1145/3397191>
- Newman M E J (2001) The structure of scientific collaboration networks. *P Natl Acad Sci* 98(2):404-409. <https://doi.org/10.1073/pnas.98.2.404>
- Girvan M, Newman M E J (2002) Community structure in social and biological networks. *P Natl Acad Sci* 99(12): 7821-7826. <https://doi.org/10.1073/pnas.122653799>
- Williams R J, Martinez N D (2000) Simple rules yield complex food webs. *Nature* 404(6774): 180-183. <https://doi.org/10.1038/35004572>
- Krause A E, Frank K A, Mason D M et al (2003) Compartments revealed in food-web structure. *Nature* 426(6964): 282-285. <https://doi.org/10.1038/nature02115>
- Jeong H, Tombor B, Albert R (2000) The large-scale organization of metabolic networks. *Nature* 407(6804): 651-654. <https://doi.org/10.1038/35036627>
- Faloutsos M, Faloutsos P, Faloutsos C (1999) On power-law relationships of the internet topology. *Comput Commun Rev* 29(4): 251-262. <https://doi.org/10.1145/316194.316229>
- Newman M E J (2004) Coauthorship networks and patterns of scientific collaboration. *P Natl Acad Sci* 101(suppl_1): 5200-5205. <https://doi.org/10.1073/pnas.0307545100>
- Papadopoulos S, Kompatsiaris Y, Vakali A et al (2012) Community detection in social media: Performance and application considerations. *Data Min Knowl Disc* 24: 515-554. <https://doi.org/10.1007/s10618-011-0224-z>
- Rostami M, Oussalah M, Berahmand K (2023) Community detection algorithms in healthcare applications: a systematic review. *IEEE Access* 11: 30247-30272. <https://doi.org/10.1109/ACCESS.2023.3260652>

11. Kumar R, Raghavan P, Rajagopalan S (1999) Trawling the web for emerging cyber-communities. *Comput Netw* 31(11-16): 1481-1493. [https://doi.org/10.1016/S1389-1286\(99\)00040-7](https://doi.org/10.1016/S1389-1286(99)00040-7)
12. Flake G W, Lawrence S, Giles C L (2000) Efficient identification of web communities. In proceedings of the sixth ACM SIGKDD international conference on Knowledge discovery and data mining 2000: 150-160. <https://doi.org/10.1145/347090.347121>
13. Steenstrup M (2001) Cluster-based networks. In: *Ad hoc networking*, Addison-Wesley Longman Publishing Co., Inc., USA, 75–138.
14. Wu A Y, Garland M, Han J (2004) Mining scale-free networks using geodesic clustering. In proceedings of the tenth ACM SIGKDD international conference on Knowledge discovery and data mining 2004: 719-724. <https://doi.org/10.1145/1014052.1014146>
15. Schaeffer S E (2007) Survey: Graph clustering. *Comput Sci Rev* 1(1): 27-64. <https://doi.org/10.1016/j.cosrev.2007.05.001>
16. Hastie T, Tibshirani R, Friedman J (2009) *The Elements of Statistical Learning, Second Edition: Data Mining, Inference, and Prediction*. New York: springer.
17. Miasnikof P, Bagherbeik M, Sheikholeslami A (2024) Graph clustering with Boltzmann machines. *Discret Appl Math* 343: 208-223. <https://doi.org/10.1016/j.dam.2023.10.012>
18. Spielman D A, Teng S H (1996) Spectral partitioning works: Planar graphs and finite element meshes. In proceedings of 37th conference on foundations of computer science IEEE 1996: 96-105. <https://doi.org/10.1109/SFCS.1996.548468>
19. Von Luxburg U (2007) A tutorial on spectral clustering. *Stat Comput* 17: 395-416. <https://doi.org/10.1007/s11222-007-9033-z>
20. Van Dongen S (2000) *Graph Clustering by Flow Simulation* (Ph.D. thesis). Faculteit Wiskunde en Informatica, Universiteit Utrecht.
21. Hofman J M, Wiggins C H (2008) Bayesian Approach to Network Modularity. *Phys Rev Lett* 100(25): 258701. <https://doi.org/10.1103/PhysRevLett.100.258701>
22. Mackay D J C (2003) *Information Theory, Inference, and Learning Algorithms*. Cambridge University Press, Cambridge, UK.
23. Jeub L G S, Balachandran P, Porter M A et al (2015) Think locally, act locally: Detection of small, medium-sized, and large communities in large networks. *Phys Rev E* 91(1): 012821. <https://doi.org/10.1103/PhysRevE.91.012821>
24. Ronhovde P, Nussinov Z (2010) Local resolution-limit-free potts model for community detection. *Phys Rev E* 81(4): 046114. <https://doi.org/10.1103/PhysRevE.81.046114>
25. Traag V A, Van Dooren P, Nesterov Y (2011) Narrow scope for resolution-limit-free community detection. *Phys Rev E* 84(1): 016114. <https://doi.org/10.1103/PhysRevE.84.016114>
26. Boccaletti S, Ivanchenko M, Latora V (2007) Detecting complex network modularity by dynamical clustering. *Phys Rev E* 75(4): 045102. <https://doi.org/10.1103/PhysRevE.75.045102>
27. Newman M E J, Girvan M (2004) Finding and evaluating community structure in networks. *Phys Rev E* 69(2): 026113. <https://doi.org/10.1103/PhysRevE.69.026113>
28. Fortunato S, Latora V, Marchiori M (2004) Method to find community structures based on information centrality. *Phys Rev E* 70(5): 056104. <https://doi.org/10.1103/PhysRevE.70.056104>
29. Hagberg A, Swart P J, Schult D A (2008) *Exploring network structure, dynamics, and function using NetworkX*. Los Alamos National Laboratory (LANL), Los Alamos, NM (United States).
30. Condon A, Karp R M (2001) Algorithms for graph partitioning on the planted partition model. *Random Struct Algorithms* 18(2): 116-140. [https://doi.org/10.1002/1098-2418\(200103\)18:2<116::AID-RSA1001>3.0.CO;2-2](https://doi.org/10.1002/1098-2418(200103)18:2<116::AID-RSA1001>3.0.CO;2-2)
31. Fan N, Pardalos P M (2010) Linear and quadratic programming approaches for the general graph partitioning problem. *J Global Optim* 48(1): 57-71. <https://doi.org/10.1007/s10898-009-9520-1>
32. Fortunato S (2010) Community detection in graphs. *Phys Rep* 486(3-5): 75-174. <https://doi.org/10.1016/j.physrep.2009.11.002>

33. Fortunato S, Hric D (2016) Community detection in networks: A user guide. *Phys Rep* 659: 1-44. <https://doi.org/10.1016/j.physrep.2016.09.002>
34. Blondel V D, Guillaume J L, Lambiotte R et al (2008) Fast unfolding of communities in large networks. *J Stat Mech-Theory Exp* 2008(10): P10008. <https://doi.org/10.1088/1742-5468/ad6139>
35. Fortunato S, Barthelemy (2007) Resolution limit in community detection. In proceedings of the national academy of sciences, 104(1): 36-41. <https://doi.org/10.1073/pnas.0605965104>
36. Good B H, De Montjoye Y A, Clauset A (2010) Performance of modularity maximization in practical contexts. *Phys Rev E* 81(4): 046106. <https://doi.org/10.1103/PhysRevE.81.046106>
37. Holland P W, Laskey K B, Leinhardt S (1983) Stochastic blockmodels: First steps. *Soc Networks* 5(2): 109-137. [https://doi.org/10.1016/0378-8733\(83\)90021-7](https://doi.org/10.1016/0378-8733(83)90021-7)
38. Wolsey L A (2020) Integer programming. John Wiley & Sons.
39. Miasnikof P, Shestopaloff A Y, Bonner A J et al (2018) A statistical performance analysis of graph clustering algorithms. In: Algorithms and Models for the Web Graph: 15th International Workshop, WAW 2018, Moscow, Russia, May 17-18, 2018, Proceedings 15. Springer International Publishing, pp 170-184.
40. Fan N, Zheng Q P, Pardalos P M (2012) Robust optimization of graph partitioning involving interval uncertainty. *Theoret Comput Sci* 447: 53-61. <https://doi.org/10.1016/j.tcs.2011.10.015>
41. Miasnikof P, Pitsoulis L, Bonner A J et al (2020) Graph clustering via intra-cluster density maximization. In: Network Algorithms, Data Mining, and Applications: NET, Moscow, Russia, May 2018 8. Springer International Publishing, pp 37-48.
42. Ponomarenko A, Pitsoulis L, Shamshetdinov M (2021) Overlapping community detection in networks based on link partitioning and partitioning around medoids. *PLoS One* 16(8): e0255717. <https://doi.org/10.1371/journal.pone.0255717>
43. Zhao P F, Li Q N, Chen W K, et al (2021) An efficient quadratic programming relaxation based algorithm for large-scale MIMO detection. *SIAM J Optim* 31(2): 1519-1545. <https://doi.org/10.1137/20M1346912>
44. Cui C, Li Q, Qi L, et al (2018) A quadratic penalty method for hypergraph matching. *J Glob Optim* 70: 237-259. <https://doi.org/10.1007/s10898-017-0583-0>
45. Miasnikof P, Shestopaloff A Y, Bonner A J et al (2020) A density-based statistical analysis of graph clustering algorithm performance. *J Complex Netw* 8(3): cnaa012. <https://doi.org/10.1093/comnet/cnaa012>
46. Miasnikof P, Shestopaloff A Y, Bonner A J et al (2018) A statistical performance analysis of graph clustering algorithms. In: Algorithms and Models for the Web Graph: 15th International Workshop, WAW 2018, Moscow, Russia, May 17-18, 2018, Proceedings 15. Springer International Publishing, pp 170-184.
47. Newman M E J (2004) Analysis of weighted networks. *Phys Rev E* 70(5): 056131. <https://doi.org/10.1103/PhysRevE.70.056131>
48. Burt R S (1976) Positions in networks. *Social forces* 55(1): 93-122. <https://doi.org/10.1093/sf/55.1.93>
49. Jaccard P (1901) étude de la distribution florale dans une portion des Alpes et du Jura. *Bull Soc Vaudoise Sci Nat* 37: 547-579.
50. Camby É, Caporossi G (2017) The extended Jaccard distance in complex networks. GERAD, École des hautes études commerciales.
51. Miasnikof P, Shestopaloff A Y, Pitsoulis L et al (2022) An empirical comparison of connectivity-based distances on a graph and their computational scalability. *J Complex Netw* 10(1): cnac003. <https://doi.org/10.1093/comnet/cnac003>
52. Miasnikof P, Shestopaloff A Y, Pitsoulis L et al (2021) Distances on a graph. In: Complex Networks & Their Applications IX: Volume 1, Proceedings of the Ninth International Conference on Complex Networks and Their Applications COMPLEX NETWORKS 2020. Springer International Publishing, pp 189-199.

53. Garcia-Mendez S, Fernandez-Gavilanes M, Juncal-Martinez J et al (2020) Identifying banking transaction descriptions via support vector machine short-text classification based on a specialized labelled corpus. *IEEE Access* 8(2020): 61642-61655. <https://doi.org/10.1109/ACCESS.2020.2983584>
54. Wang Z B, Cui J, Zhu Y (2020) Plant recognition based on Jaccard distance and BOW. *Multimedia Syst* 26(5): 495-508. <https://doi.org/10.1007/s00530-020-00657-6>
55. Ochiai A (1957) Zoogeographical studies on the soleoid fishes found in japan and its neighbouring regions-i. *NIPPON SUISAN GAKKAISHI* 22(9): 522-525.
56. Nocedal J, Wright S (2006) *Numerical Optimization*. Springer, Berlin.
57. Sun W, Yuan Y X (2006) *Optimization theory and methods: nonlinear programming*. Springer Science & Business Media, New York.
58. Gurobi Optimization, LLC, *Gurobi Optimizer Reference Manual*. 2023. [Online]. Available: <https://www.gurobi.com>